

# 펠라듐과 테루리움계의 상평형 연구

김 원 사\* · G. Y. Chao \*\* and L. J. Cabri \*\*\*

\* 충남대학교 자연과학대학 지질학과

\*\* 칼튼대학교 지질학과

\*\*\* 캐나다 광물에너지 연구소

## Phase Constitution of the Palladium and Tellurium System

Won-Sa Kim\*, G. Y. Chao\*\*, and L. J. Cabri\*\*\*

\* Department of Geology, Chungnam National University, Daejeon 305-764, Korea

\*\* Department of Earth Sciences, Carleton University, Ottawa, Ontario K1S 5B6, Canada

\*\*\* Canada Centre for Mineral and Energy Technology, 555 Booth Street, Ottawa, Ontario K1A 0G1, Canada

### 요 약

Pd-Te계의 상평형도를 시차열분석, X선회절분석, 전자현미분석, 반사현미경을 사용해 연구하였다. 본 계의 0-50 at.%Te 부분의 새로운 상관계가 정립되었다. 본 계에는 Pd<sub>17</sub>Te<sub>4</sub>, Pd<sub>20</sub>Te<sub>7</sub>, Pd<sub>8</sub>Te<sub>3</sub>, Pd<sub>7</sub>Te<sub>3</sub>, Pd<sub>6</sub>Te<sub>4</sub>, Pd<sub>3</sub>Te<sub>2</sub>, PdTe, PdTe<sub>2</sub> 등 8개의 화합물이 존재하며 이중 Pd<sub>17</sub>Te<sub>4</sub>와 Pd<sub>7</sub>Te<sub>3</sub>는 처음 보고되는 신종 화합물이다.

Pd<sub>17</sub>Te<sub>4</sub>는 등축정계이며 공간군 Fd3c에 속하며 단위포 크기(a)는 12.678(5)Å이다. Pd<sub>8</sub>Te<sub>3</sub>와 Pd<sub>7</sub>Te<sub>3</sub>의 X선회절분말자료는 사방정계의 단위포 a=12.843(3), b=15.126(3), c=11.304(2)Å와 단사정계의 단위포 a=7.444(1), b=13.918(2), c=8.873(2)Å, β=92.46(2)°에 의해 각각 격자지수화가 가능하였다. 본계에 존재하는 합성 화합물의 일부 물리적, 광학적 자료를 새로 보고하였다.

### Abstract

The Pd-Te system has been investigated by differential thermal analysis, X-ray diffraction, electron probe microanalysis and reflected light microscopy. New phase relations in 0-50 at.% Te portion of the binary system are proposed. Eight binary phases exist in the

system: Pd<sub>17</sub>Te<sub>4</sub>, Pd<sub>20</sub>Te<sub>7</sub>, Pd<sub>8</sub>Te<sub>3</sub>, Pd<sub>7</sub>Te<sub>3</sub>, Pd<sub>6</sub>Te<sub>4</sub>, Pd<sub>3</sub>Te<sub>2</sub>, PdTe and PdTe<sub>2</sub>. Of these, Pd<sub>7</sub>Te<sub>3</sub> is a newly reported phase. Pd<sub>17</sub>Te<sub>4</sub> is cubic, space group Fd3c, with a=12.678(5)Å. The X-ray powder data of Pd<sub>8</sub>Te<sub>3</sub>, indexed on an orthorhombic cell, give a=12.843(3), b=15.126(3), c=11.304(2)Å and those of Pd<sub>7</sub>Te<sub>3</sub>, indexed on a monoclinic cell, give a=7.444(1), b=13.918(2), c=8.873(2)Å. β=92.46(2)°. Some physical and optical properties of synthetic phases in the system are also reported.

### INTRODUCTION

The phase diagram of the Pd-Te system by Medvedeva et al.<sup>1)</sup> for the range between 20 and 100 at.% Te illustrates the phase relations among six previously reported phases: Pd<sub>4</sub>Te, Pd<sub>3</sub>Te, Pd<sub>5</sub>Te<sub>2</sub> and Pd<sub>2</sub>Te<sup>2)</sup>; PdTe<sup>3)</sup>; and PdTe<sub>2</sub><sup>4)</sup>. Phase relations between PdTe and PdTe<sub>2</sub> were reinvestigated by Kjekshus and Pearson<sup>5)</sup> and Hoffman and MacLean<sup>6)</sup> partly because the field bounded by the liquidus and solidus curves of the PdTe and PdTe<sub>2</sub> phases in Medvedeva et al.'s diagram is a 3-phase area(PdTe+PdTe<sub>2</sub>+liquid), violating the Phase Rule, as pointed out by Elliott<sup>7)</sup>. Kjekshus and Pearson<sup>5)</sup> found a continuous solid solution

between PdTe and PdTe<sub>2</sub> above 660–670°C and restricted homogeneity ranges for the PdTe and PdTe<sub>2</sub> phases at lower temperatures (probably below 500°C). Hoffman and MacLean<sup>6)</sup> reported that, between 575±10°C and 710°C±10°C, PdTe and PdTe<sub>2</sub> formed a complete solid solution which was unquenchable; below 570°C±10°C, PdTe and PdTe<sub>2</sub> occur as distinct phases.

The problematic phase relation in the Pd–Te phase diagram were further increased as more phases such as Pd<sub>3</sub>Te<sub>2</sub><sup>8)</sup>, Pd<sub>20</sub>Te<sub>7</sub><sup>9)</sup>, Pd<sub>9</sub>Te<sub>4</sub><sup>10)</sup>, and Pd<sub>8</sub>Te<sub>3</sub><sup>11)</sup>, were reported since Medvedeva et al.<sup>1)</sup> published their phase diagram. Furthermore, 2 different phase diagrams have recently been published for the composition range 0–50 at.% Te and 20–100 at.% Te, based mainly on the thermal data, by Chattopadhyay et al.<sup>12)</sup> and Ipsier and Schuster<sup>13)</sup>, respectively. They also include a few high temperature phases:  $\gamma$  (Pd<sub>3</sub>Te),  $\delta$  and  $\delta'$ <sup>12)</sup>;  $\xi$ <sup>13)</sup>.

In view of the above new and sometimes conflicting data, it was felt that the Pd–Te phase diagram merited reinvestigation. A special emphasis was made in the region from 0–50 at.% Te because the composition of all the newly reported Pd–Te phases fall in that region and considerable uncertainties remain in the phase relations.

## EXPERIMENTAL DETAILS

Mixes were prepared from palladium wire and sponge (99.999% purity) and spectrographically pure tellurium ingot, all purchased from the Johnson Matthey Chemical Ltd., and sealed in evacuated silica glass tubes. The capsules were placed in horizontal muffle furnaces and heated at selected temperatures. To ensure homogeneity most samples were opened, after initial heating, ground under acetone, pelletized and re-loaded in the furnaces for a further heating period. The total heating period ranges from a few days to nearly 5 months. Experimental runs were rapidly removed from the furnace and quenched by dropping them in ice water.

Run products were studied by reflected light micros-

copy, X-ray diffraction, and electron probe microanalysis. X-ray powder diffraction patterns were obtained with 114.6mm Gandolfi cameras using Ni-filtered CuK $\alpha$  radiation. When more accurate X-ray data were required for calculation of the cell dimensions, a Philips automated X-ray diffractometer and monochromatized CuK $\alpha$  radiation were used. Single crystals were analysed with a precession camera.

Compositions of individual phases in each run product were determined with a Cambridge MK5 electron microprobe analyser using homogeneous synthetic Pd–Te compounds and spectrographically pure Pd and Te elements as standards. Errors of microprobe analyses are approximately ±1% of major elements present.

For the differential thermal analyses, samples of approximately 0.2g were evacuated and sealed in small silica tubes with a tiny thermocouple well in one end. An identical tube held the reference material,  $\alpha$ –Al<sub>2</sub>O<sub>3</sub>. The sample and reference containers were placed on the ends of Pt/Pt 15%Rh thermocouples which were positioned vertically about 2 cm apart inside a electrically heated furnace. Heating rates of 6 and 12°C/min were used. A total of 29 samples was analysed by DTA.

Micro-indentation hardness was measured for the synthetic phases using a Leitz DURIMET small-hardness tester.

## RESULTS

Experimental data for the runs (starting compositions, reaction products and their microprobe analyses) are lengthy and omitted here (however, they are available through authors upon request). The Pd–Te phase diagram (Fig. 1) is based on these experimental results and DTA data obtained on heating performed in this study. The existence of Pd<sub>17</sub>Te<sub>4</sub> (or “Pd<sub>4</sub>Te”), Pd<sub>20</sub>Te<sub>7</sub>, Pd<sub>8</sub>Te<sub>3</sub>, Pd<sub>9</sub>Te<sub>4</sub>, Pd<sub>3</sub>Te<sub>2</sub>, PdTe, and PdTe<sub>2</sub> is confirmed and a new phase, Pd<sub>7</sub>Te<sub>3</sub>, is encountered in this study.

Palladium in reaction products, quenched from 700°C, 800°C and 1000°C, contains respectively 13.4–13.7at.% Te(runs 849 and 848), 14.8 at.% Te(run 79–2) and 10.8 at.% Te(runs 79–1 and 79–3) in solid solution.

The composition of the phase that is identical, according to X-ray diffraction, to the Pd<sub>4</sub>Te phase of Gronvold and Rost<sup>2)</sup> is determined to be 19.0±0.4 at.% Te. The formula of the phase is, therefore, revised to Pd<sub>17</sub>Te<sub>4</sub> as it is deemed to better represent the composition. Under reflected light, Pd<sub>17</sub>Te<sub>4</sub> is light pinkish grey in air and in oil. The micro-indentation hardness value is VHN<sub>100</sub>=259(234–289) for four indentations. Single crystal precession photographs for Pd<sub>17</sub>Te<sub>4</sub>, quenched from 700°C after 5 months annealing period, show cubic symmetry with space group Fd3c. The cell parameter as refined by a least-squares method, using X-ray powder diffraction data (Table 1), is 12.678(5)Å, in good agreement with a=12.674Å given by Gronvold and Rost<sup>2)</sup>.

The Pd<sub>20</sub>Te<sub>7</sub> phase of Wopersnow and Schubert<sup>9)</sup> (formerly known as Pd<sub>3</sub>Te<sup>2)</sup>) is confirmed. DTA data show that Pd<sub>20</sub>Te<sub>7</sub> undergoes a transformation at 745°C before it melts incongruently at 885°C. The high temperature structure is apparently not quenchable as the phase quenched from temperatures above and below the transition point give identical X-ray powder diffraction patterns. Lamellar twinning, most likely a product of quenching through the phase-transformation, is common in the single-phased Pd<sub>20</sub>Te<sub>7</sub> products(runs 802, 822 and 837). The X-ray powder pattern of Pd<sub>20</sub>Te<sub>7</sub> synthesized in this study is indexed according to Wopersnow and Schubert<sup>9)</sup> and the cell parameters, refined by least-squares method, are a=11.797(3), c=11.150(4)Å, in good agreement with a=11.797(1), c=11.172(2)Å reported by Wopersnow and Schubert<sup>9)</sup>. Under reflected light, Pd<sub>20</sub>Te<sub>7</sub> is cream colored in air and in oil, and is non-birefractant. Anisotropism varies from weak(dark grey to extinction)to strong(orange brown to deep blue) in air and in oil Micro-indentation hardness measurements give VHN<sub>100</sub>=515(488–548) for five indentations.

Table 1. X-ray powder diffraction data for synthetic Pd<sub>17</sub>Te<sub>4</sub> and Pd<sub>4</sub>Te

Pd <sub>17</sub> Te <sub>4</sub> <sup>(1)</sup>		Pd <sub>4</sub> Te <sup>(2)</sup>		
d <sub>o</sub> (Å)	I/I <sub>o</sub>	d <sub>o</sub> (Å)	I/I <sub>o</sub>	h <sup>2</sup> +k <sup>2</sup> +l <sup>2</sup>
2.435	15	2.435	vw	27
		2.273	vw	?
2.231	100	2.231	vst	32
		1.971	vw	41
1.645	20	1.646	w	59
1.579	40	1.581	m	64
		1.392	vw	83
		1.375	vw	85
1.291	70	1.292	st	96
1.223	20	1.224	w	107
		1.190	vw	113
		1.172	vw	117
1.119	40	1.148	vw	122
		1.120	m	128
1.000	20	1.074	vw	139
		1.001	m	160
0.968	20	0.968	w	171
Plus 17 lines				

(1) This study, Run 848(Pd+Pd<sub>17</sub>Te<sub>4</sub>), quenched from 700°C. CuK<sub>α</sub> radiation, 114.6mm Gandolfi camera. a=12.678(5)Å.

(2) Gronvold and Røst(1956). Heated at 500°C. CuK<sub>α</sub> radiation, 114.6mm camera. D - values converted from their θ values. a =12.674Å. w:weak. m:medium. st:strong.

The eutectic point between Pd<sub>17</sub>Te<sub>4</sub> and Pd<sub>20</sub>Te<sub>7</sub> is placed at 23.5 at.% Te, 720°C, as determined by DTA, compared to previous data of Chattopadhyay<sup>12)</sup>:780°C between the α and γ phases.

Pd<sub>8</sub>Te<sub>3</sub>, whose existence was first reported by Cabri et al.<sup>11)</sup> is confirmed and found to have a composition

Table 2. X-ray powder diffraction data of synthetic Pd<sub>8</sub>Te<sub>3</sub>

(1)					(2)		
h	k	l	d <sub>c</sub> (Å)	d <sub>c</sub> (Å)	I/I <sub>0</sub>	d <sub>c</sub> (Å)	I/I <sub>0</sub>
1	4	0	3.627	3.636	8	3.568	1
2	3	2	3.246	3.244	2	2.879	1
2	2	3	2.986		10	2.487	1
4	2	0	2.956	2.978		2.447	1
1	3	3	2.938	2.937	10	2.280	1
3	0	3	2.829	2.831	4	2.250	10
4	3	0	2.709	2.691	11	2.184	1
5	0	1	2.505	2.506	12	2.128	1
4	3	2	2.443	2.440	37	2.052	1
2	6	0	2.346	2.346	42	1.976	1
4	2	3	2.326	2.328	33	1.934	1
0	0	5	2.260	2.261	75	1.885	1
2	5	3	2.215	2.218	53	1.865	1
2	6	0	2.172	2.177	100	1.783	1
3	6	2	2.027	2.028	2	1.713	1
4	6	0	1.983	1.983	5	1.633	1
4	6	1	1.953	1.952	14	1.569	1
2	7	2	1.925	1.923	23	1.475	1
1	5	5	1.793	1.793	10	1.449	1
7	2	1	1.761	1.761	7	1.424	1
4	0	6	1.625	1.625	4	1.392	1
8	1	1	1.581	1.583	4	1.343	1
3	7	5	1.467	1.468	11	1.329	1
4	5	6	1.431	1.432	4	1.317	1
1	11	0	1.367		7	1.277	1
5	0	7	1.367	1.367			
2	11	0	1.344	1.344	8	1.264	1
7	6	4	1.313	1.314	14	1.245	1
9	6	0	1.2422	1.2427	24	1.227	1
2	11	4	1.2142	1.2147	3	1.218	1
2	3	9	1.1974	1.1975	5	1.208	1

(1) Run 841, quenched from 800°C and allowed to

re-equilibrate at room temperature CuK<sub>α1</sub> radiation ( $\lambda = 1.54059\text{Å}$ ), automated diffractometer. Indexed on an orthorhombic cell with  $a=12.843(3)$ ,  $b=15.126(3)$ ,  $c=11.304(2)\text{Å}$ (2) Run850, quenched from 500°C. CuK<sub>α</sub> radiation ( $\lambda = 1.5418\text{Å}$ ), 114.6mm Gandolfi camera. Not indexed.

of 27.3 at.% Te with no detectable composition range. DTA data show two endothermic reactions at 270°C and 680°C before it melts congruently at 900°C: these are interpreted as polymorphic transformations. It is noted that lamellar twinning, frequently observed in the quenched Pd<sub>8</sub>Te<sub>3</sub> grains, may be suggestive of the phase transformation involved. Gandolfi X-ray powder patterns of Pd<sub>8</sub>Te<sub>3</sub> quenched from 800°C (Table 2), 640°C, 600°C and 410°C and allowed to re-equilibrate at room temperature are all identical. An X-ray powder pattern obtained immediately after quenching from 500°C, however, is different (Table 2) and is interpreted as the intermediate temperature form of Pd<sub>8</sub>Te<sub>3</sub>. The X-ray powder pattern (Table 2) of Pd<sub>8</sub>Te<sub>3</sub>, quenched from 800°C, is indexed on an orthorhombic cell with  $a = 12.843(3)$ ,  $b = 15.126(3)$ ,  $c = 11.304(2)\text{Å}$ . Pd<sub>8</sub>Te<sub>3</sub> is creamy yellow or pale grey, under reflected light, in air and in oil with weak to moderate birefractance. It is strongly anisotropic from dark greyish blue to pale orange in air and slightly stronger in oil. Micro-indentation hardness value was not measured because of the lamellar twinning present in the quenched phase. Cabri<sup>(14)</sup> reported an unnamed mineral with Pd<sub>8</sub>Te<sub>3</sub> composition.

Pd<sub>7</sub>Te<sub>3</sub>, 29.5±0.5 at.% Te in composition, synthesized between 410° and 800°C, is a previously unreported phase. The formula Pd<sub>7</sub>Te<sub>3</sub> is established by the electron microprobe data for runs (75, 844 and 846) quenched from the Pd<sub>7</sub>Te<sub>3</sub> + liquid field as the composition is variable in the Pd<sub>7</sub>Te<sub>3</sub> + Pd<sub>8</sub>Te<sub>3</sub> field. The phase with Pd<sub>5</sub>Te<sub>2</sub> stoichiometry<sup>2)</sup> was not found. According to our DTA data Pd<sub>7</sub>Te<sub>3</sub> shows thermal effects at 470°, 595°C, and 830°C. It is not certain whether the first two are due to transformation, although the last is interpreted as melting. It is noted

that a few additional thermal effects, not shown in Fig. 1, are observed for the area between Pd<sub>8</sub>Te<sub>3</sub> and Pd<sub>7</sub>Te<sub>3</sub>; 270°C; 330°C; 490°C and 555°C. They are very difficult to interpret. The X-ray powder diffraction pattern (Table 3) of the Pd<sub>7</sub>Te<sub>3</sub> phase is not identical, but closely related to that of the Pd<sub>9</sub>Te<sub>4</sub> phase<sup>10</sup>. The

X-ray powder data is thus indexed on the monoclinic cell of Pd<sub>9</sub>Te<sub>4</sub><sup>10</sup> and the refined cell parameters are a = 7.444(1), b = 13.918(2), c = 8.873(2) Å, β = 92.46(2)°. Under reflected light Pd<sub>7</sub>Te<sub>3</sub> is greyish pink in air and in oil, and is weakly birefractant. It is weakly anisotropic from greyish brown with a red tinge to extinction in air and slightly stronger in oil.

Table 3. X-ray powder diffraction data of synthetic Pd<sub>7</sub>Te<sub>3</sub>

h	k	l	d(Å)	d(Å)	I/I <sub>0</sub>	h	k	l	d <sub>0</sub> (Å)	d <sub>0</sub> (Å)	I/I <sub>0</sub>
2	2	$\bar{1}$	3.114	3.127	8	3	5	1	1.800		
1	3	$\bar{2}$	2.977	2.974	4	1	4	4	1.797	1.798	4
2	1	$\bar{2}$	2.849	2.849	6	3	2	3	1.797		
2	3	$\bar{1}$	2.785	2.788	6	4	1	$\bar{3}$	1.594	1.595	9
0	4	$\bar{2}$	2.737	2.740	8	0	1	6	1.469	1.469	4
2	3	1	2.730	2.728	13	5	1	$\bar{1}$	1.469		
1	4	2	2.546	2.545	14	1	0	6	1.437	1.437	2
3	0	0	2.479	2.478	8	2	5	$\bar{5}$	1.405	1.404	8
2	3	$\bar{2}$	2.465	2.465	15	2	7	$\bar{4}$	1.388		4
3	0	$\bar{1}$	2.414	2.412	7	3	7	$\bar{3}$	1.388	1.388	
1	5	2	2.232	2.233	100	4	3	$\bar{4}$	1.388		
0	0	4	2.216	2.217	90	4	7	$\bar{1}$	1.348	1.349	3
0	1	4	2.188	2.191	30	1	10	2	1.304	1.304	16
1	0	4	2.149	2.150	16	4	8	$\bar{1}$	1.262	1.263	6
3	0	2	2.125	2.128	20	4	5	4	1.247	1.247	4
1	0	$\bar{4}$	2.099	2.099	18	3	2	6	1.226	1.226	5
0	6	2	2.055	2.061	6	1	8	5	1.218	1.218	4
3	2	2	2.032	2.031	6	1	12	$\bar{1}$	1.137	1.137	3
0	7	0	1.988	1.988	14	0	6	7	1.111	1.111	5
2	6	0	1.968	1.967	12	5	8	$\bar{2}$	1.104	1.104	4
2	6	$\bar{1}$	1.930	1.931	8	3	5	$\bar{7}$	1.061	1.061	2
1	7	$\bar{1}$	1.872								
2	2	$\bar{4}$	1.869								
3	2	$\bar{3}$	1.869	1.870	12						
0	4	4	1.869								
2	0	4	1.868								

Run 808, quenched from 600°C. CuK<sub>α1</sub> radiation (λ = 1.54059 Å), automated diffractometer. Indexed on a monoclinic cell with a = 7.444(1), b = 13.918(2), c = 8.873(2) Å, β = 92.46(2)°.

The  $\text{Pd}_3\text{Te}_4$  phase first reported by Matkovic and Schubert<sup>10)</sup> is confirmed, whereas the  $\text{Pd}_2\text{Te}$  phase<sup>2)</sup> was not found. From the X-ray diffraction data there is little doubt that the  $\text{Pd}_2\text{Te}$  phase is structurally the same as  $\text{Pd}_3\text{Te}_4$ . According to DTA data,  $\text{Pd}_3\text{Te}_4$  may undergo a polymorphic transformation at 462°C and melts incongruently at 605°C to form  $\text{Pd}_7\text{Te}_3$  and liquid of composition about 65 at.% Pd.

X-ray powder patterns of the  $\text{Pd}_3\text{Te}_4$  phase, quenched from above and below the phase transformation temperature (462°C), are identical, suggesting that the high-temperature structure is not quenchable. The refined cell parameters, using the present X-ray powder data, are  $a=7.449(1)$ ,  $b=13.916(3)$ ,  $c=8.841(4)\text{Å}$ ,  $\beta=92.01(5)^\circ$ , in agreement with those reported by Matkovic and Schubert<sup>10)</sup> and Cabri et al.<sup>11)</sup>. Under reflected light  $\text{Pd}_3\text{Te}_4$  is pinkish grey or cream colored in air and in oil. It is very weakly birefractant from pinkish brown to creamy yellow, and moderately anisotropic from grey to extinction. Micro-indentation hardness values are  $\text{VHN}_{100}=176(146-210)$ . These optical and physical properties are similar to those for the mineral tellurpalladinite of the same composition<sup>11)</sup>.

$\text{Pd}_3\text{Te}_2$  was first synthesized by El-Boragy and Schubert<sup>9)</sup>, and Matkovic and Schubert<sup>15)</sup> reported it to be stable at least up to 480°C. The  $\text{Pd}_3\text{Te}_2$  phase is confirmed and DTA data show endothermic reactions at 462°C and 504°C. The X-ray powder pattern of the  $\text{Pd}_3\text{Te}_2$  phase synthesized at 450°C in this study is indexed according to the orthorhombic cell of Matkovic and Schubert<sup>15)</sup> with cell parameters  $a=7.875(2)$ ,  $b=12.675(4)$ ,  $c=3.853(1)\text{Å}$ . Under reflected light  $\text{Pd}_3\text{Te}_2$  is pale pinkish brown with a grey tint in air. It is very weakly birefractant and weakly anisotropic from greyish brown to grey in air. Micro-indentation hardness tests give  $\text{VHN}_{15}=275(257-290)$  for four indentations.

A eutectic point between  $\text{Pd}_3\text{Te}_4$  and  $\text{Pd}_3\text{Te}_2$  is located at about 39 at.% Te and 498°C.

$\text{PdTe}$  is synthesized between 400°C and 700°C in this study. Electron microprobe analyses show that  $\text{PdTe}$  synthesized below 450°C has a 1:1 ratio, whereas when

synthesized at or above 500°C it becomes slightly depleted in Pd with increasing temperature: 50.4 at.% at 500°C; 51.0 at.% at 600°C; and 51.8 at.% Te at 700°C. The cell dimensions of the  $\text{PdTe}$  phase (51.6 at.% Te, run 820) synthesized at 600°C, refined by a least-squares method using the present X-ray powder data, are  $a=4.130(3)$ ,  $c=5.661(5)\text{Å}$ , in good agreement with those of Thomassen<sup>4)</sup> and Gronvold and Rost<sup>2)</sup>. Under reflected light  $\text{PdTe}$  is pale yellow in air and in oil. Birefractance of the phase is absent to very weak in air and slightly enhanced in oil. It is strongly anisotropic from dark yellow to greyish violet in air and in oil. Micro-indentation hardness values are  $\text{VHN}_{100}=197(195-198)$  for four indentations at each load.

$\text{PdTe}_2$  is synthesized in this study at temperatures between 600°C and 710°C and its cell parameters, refined by a least-squares method, are in good agreement with those reported by previous authors. Optical properties of the  $\text{PdTe}_2$  phase reported by Groeneveld Meijer<sup>16)</sup> are confirmed and micro-indentation hardness tests give  $\text{VHN}_{100}=115(110-121)$  for five indentations.

An attempt was made to confirm the existing phase relations for the area between  $\text{PdTe}$  and  $\text{PdTe}_2$  by preparing ten charges with different bulk compositions and experimental temperatures. Runs 827, 828 and 829 quenched from 710°C all yield a perthitic intergrowth of  $\text{PdTe}$  and  $\text{PdTe}_2$ . Although the runs all fell in the region between the liquidus and solidus according to the phase diagram of Medvedeva et al., the presence of a liquid phase cannot be verified due to the small grain size. Run 821, 57.5 at.% Te in bulk composition and quenched from 600°C, yields small patches of  $\text{PdTe}_2$  solid solution (containing 65.0 at.% Te) in a matrix of a fine lamellar intergrowth but  $\text{PdTe}$  and  $\text{PdTe}_2$ . These intergrowths are probably also solid solutions but are too fine-grained for analysis with the electron microprobe. Run 818, identical in bulk composition to run 821, but quenched from 670°C, resulted in coarser lamellae of  $\text{PdTe}_2$  solid solution (containing 62.5 at.% Te) in a matrix similar to that of run 821. The

texture observed from the quenched phases suggests two episodes of exsolution taking place on quenching; crystals of  $\text{PdTe}_2$  first exsolved from the  $\text{PdTe-PdTe}_2$  solid solution and subsequently, at lower temperatures, fine lamellae of  $\text{PdTe}_2$  exsolved from the remaining matrix. The exsolution curve in Medvedeva et al.<sup>1)</sup> does not explain the existence of the second exsolution phase.

## DISCUSSION

Based upon our experimental results, none of the phase diagrams proposed by Medvedeva et al.<sup>2)</sup>, Chattopadhyay et al.<sup>12)</sup>, and Ipser and Schuster<sup>13)</sup> is confirmed. Although many similarities exist between the latter two observations and ours, especially in the DTA data, our interpretation differs considerably, presumably because of our emphasis on reflecting microscopy and X-ray diffraction analysis in addition to DTA and electron probe microanalysis.

The maximum solid solubility limits of Te in Pd determined in this study are significantly different from that (12.5 at.% Te) proposed by Chattopadhyay et al.<sup>12)</sup>: 10.8 at.% Te (1000°C); 14.8 at.% Te (800°C), 13.4–13.7 at. (700%).

The composition of the phase believed to be identical to  $\text{Pd}_{17}\text{Te}_4$  (19.0±0.4 at.% Te) of this study varies with investigators: 20 at.% Te for  $\text{Pd}_4\text{Te}^2)$ ; 17.6–18.8 at.% Te for  $\text{Pd}_5\text{Te}_2$ <sup>12)</sup>; 20 at.% Te or higher in the Te content for  $\text{Pd}_4\text{Te}$ <sup>13)</sup> and 22.2 at.% Te for  $\text{Pd}_{3.5}\text{Te}$ <sup>17)</sup>. We believe that existence of  $\text{Pd}_4\text{Te}$  of stoichiometric composition is questionable.

The composition of  $\text{Pd}_{20}\text{Te}_7$  also varies with authors: 25.4–28.0 at.% Te<sup>9)</sup>; and 25.2–26.5 at.% Te<sup>12)</sup>. Our observation, however, indicates that  $\text{Pd}_{20}\text{Te}_7$  has 26.3±0.3 at.% Te with no apparent homogeneity range. Bhan and Kudielka<sup>18)</sup> observed a phase transition of  $\text{Pd}_{20}\text{Te}_7$ , at around 752°C, by high temperature X-ray diffraction, which is in good agreement with our observation (745°C).

Matkovic and Schubert<sup>10)</sup> reported the existence of a

single phase at 27 at.% Te and 410°C, which is assumed to be identical to  $\text{Pd}_8\text{Te}_3$ . The existence of  $\text{Pd}_{2.5}\text{Te}^{2), 13)}$  is not confirmed. We assume that  $\text{Pd}_{2.5}\text{Te}$  and  $\delta$  phase proposed by Chattopadhyay et al.<sup>12)</sup> might have been a mixture of  $\text{Pd}_8\text{Te}_3$  and  $\text{Pd}_7\text{Te}_3$ .  $\text{PdTe}$  is found to have a stoichiometric composition below 450°C and becomes gradually depleted in Pd with increasing temperature. The palladium-rich boundary (50.4 at.% Te) of  $\text{PdTe}$  at 500°C is in good agreement with that (50.5 at.% Te) by Kjekshus and Pearson<sup>5)</sup>. Table 4 is a summary of the phases characterized in this study and equivalent minerals found in nature.

Comparison between the earlier reported high temperature phases  $\gamma$ ,  $\delta$ ,  $\delta'$ <sup>12)</sup> and  $\xi$ <sup>13)</sup> with the phases observed in this study was not possible because of the lack in X-ray data in those papers. Because those authors report high temperature phases with relatively large homogeneity ranges, one may speculate whether the high temperature phases might have been mixtures. The  $\gamma$  phase has a composition similar to  $\text{Pd}_{20}\text{Te}_7$  and may be interpreted as the high temperature form of  $\text{Pd}_{20}\text{Te}_7$ . Its decomposition temperature (727°C) may be possibly explained by its phase transition temperature. The  $\delta$  phase (29.5–31.5 at.% Te) may be assumed to be a mixture of  $\text{Pd}_5\text{Te}_4$  and  $\text{Pd}_7\text{Te}_3$ . The thermal arrest at 610°C for this phase may be due to melting of  $\text{Pd}_5\text{Te}_4$ . The  $\delta'$  phase (25.8–29.4 at.% Te) is also assumed to be a heterogeneous mixture of  $\text{Pd}_8\text{Te}_3$  and  $\text{Pd}_{20}\text{Te}_7$  and its congruent melting (905°C at 27.2 at.% Te composition) is explained as congruent melting (900°C) of the  $\text{Pd}_8\text{Te}_3$  phase, probably the dominant phase in the mixture. The  $\xi$  phase could also have been a mixture of  $\text{Pd}_{20}\text{Te}_7$ ,  $\text{Pd}_8\text{Te}_3$ , and  $\text{Pd}_7\text{Te}_3$ . The temperature (910°C) reported for congruent melting of the phase with 28.8 at.% Te composition, may also be interpreted as the of the melting (900°C) of  $\text{Pd}_8\text{Te}_3$ , probably the major constituent in a mixture with a bulk composition of 27.8 at.% Te. However, confirmation must await until X-ray data on the high temperature phases reported by

Table 4. Summary of the phases present in the Pd-Te system

Phases	Composition (at.% Te)	Crystal structure	Lattice Parameters(Å)	Mineralogical equivalents
Pd <sub>17</sub> Te <sub>4</sub>	19.0±0.4	Cubic	a=12.678(5)	Not known <sup>a</sup>
Pd <sub>20</sub> Te <sub>7</sub>	26.3±0.3	Rhombohedral	a=11.797(3) c=11.150(4)	Not known <sup>b</sup>
Pd <sub>8</sub> Te <sub>3</sub>	27.3	Orthorhombic	a=12.843(3) b=15.126(2) c=11.304(2)	Unnamed Pd <sub>8</sub> Te <sub>3</sub> [14]
Pd <sub>7</sub> Te <sub>3</sub>	29.5±0.5	Monoclinic	a=7.444(1) b=13.918(2) c=8.873(2) β=92.46(2) <sup>o</sup>	Not known
Pd <sub>6</sub> Te <sub>4</sub>	31.2±0.4	Monoclinic	a=7.449(1) b=13.916(3) c=8.841(4) β=92.01(5) <sup>o</sup>	Telluropalladinite [11]
Pd <sub>3</sub> Te <sub>2</sub>	40.0	Orthorhombic	a=7.875(2) b=12.675(4) c=3.853(1)	Not known
PdTe	50.0—51.9	Hexagonal	a=4.130(3) <sup>c</sup> c=5.661(5)	Kotulskite [20]
PdTe <sub>2</sub>	66.7	Hexagonal	a=4.0327(6) c=5.1378(7)	Merenskyite [21]

<sup>a</sup>[19] suggests that telargpalite [22] is Pd<sub>17</sub>Te<sub>4</sub>, but the X-ray pattern of telargpalite is different from of Pd<sub>17</sub>Te<sub>4</sub>.

<sup>b</sup>[19] suggests that telargpalite [11] is Pd<sub>20</sub>Te<sub>7</sub>, but the X-ray pattern of telargpalite is different from of Pd<sub>20</sub>Te<sub>7</sub>.

<sup>c</sup>Run 820(Pd<sub>48.4</sub>Te<sub>51.6</sub>), quenched from 600°C.



Chattopadhyay et al.<sup>12)</sup> and Ipser and Schuster<sup>13)</sup> become available.

The phase relations between PdTe and PdTe<sub>2</sub>, whether a continuous solid solution exists between the two phases, are controversial. Medvedeva et al.<sup>1)</sup> reported a continuous solid solution between PdTe and PdTe<sub>2</sub> in the range 640°C–690°C, which was confirmed by Kjeshus and Pearson<sup>5)</sup>. Hoffman and MacLean<sup>6)</sup> re-confirmed the existence of the same solid solution, but at different temperatures, between 570°C±10°C and 710°C±10°C. In contrast, Ipser<sup>23)</sup>, Ipser and Schuster<sup>13)</sup>, and Mallika and Sreedharan<sup>24)</sup> carried out thermodynamic and DTA studies which excluded the possibility of PdTe–PdTe<sub>2</sub> solid solution.

However, the exsolution texture seen in run products 827, 828 and 829 cannot be explained by the phase diagram of Ipser and Schuster<sup>13)</sup> in which no exsolution is predicted. We prefer to include an exsolution curve between PdTe and PdTe<sub>2</sub> (Fig. 1), on the basis of our microscopic observations. A similar exsolution texture, consisting of a fine intergrowth of kotulskite(PdTe) and merenskyite(PdTe<sub>2</sub>), has been reported from the Merensky Reef, South Africa<sup>21)</sup> and from the Stillwater Complex, Montana<sup>25)</sup>. A more detailed reinvestigation, employing DTA, electron probe microanalysis and reflecting microscopy, is thus needed for a better understanding of the phase relations in the area.

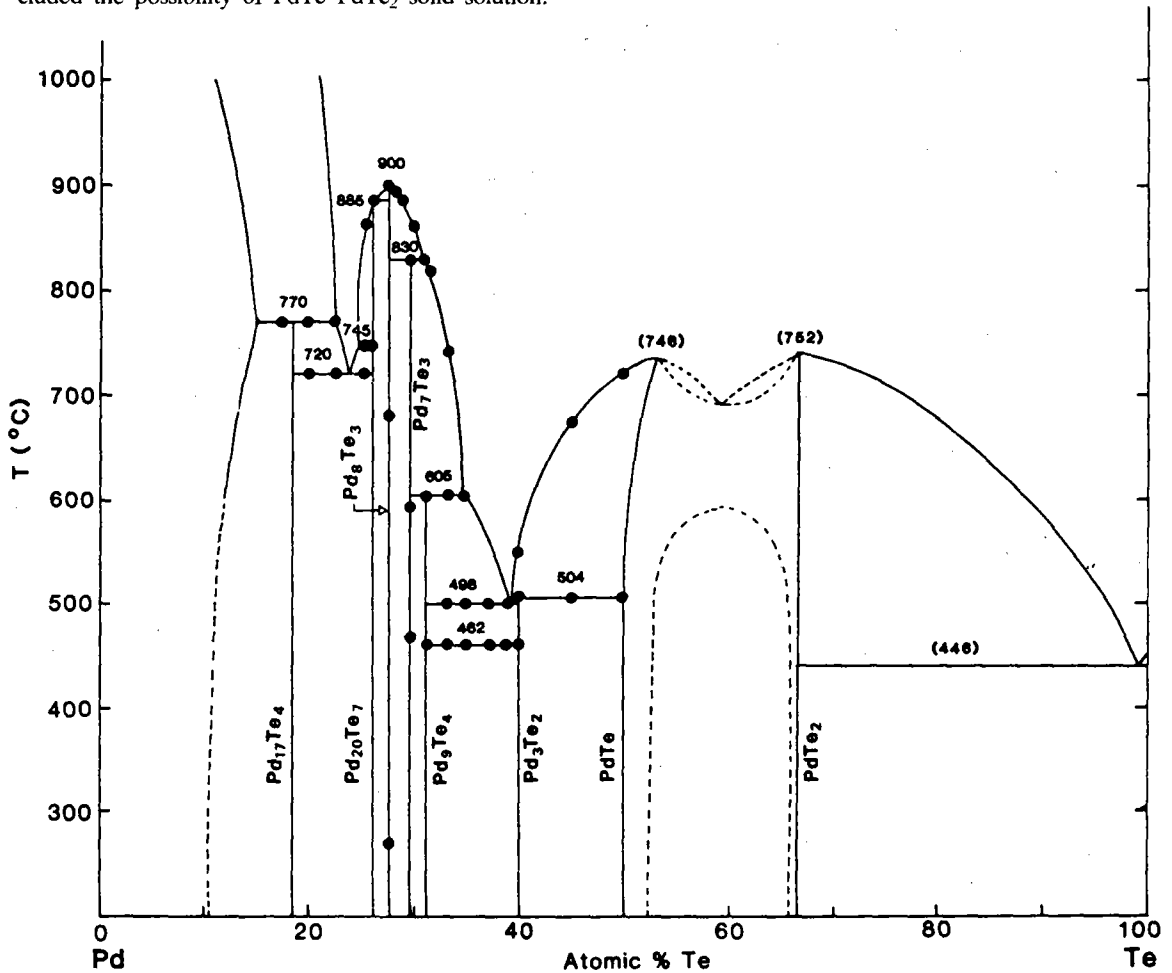


Fig. 1 Phase diagram of the Pd – Te system: ●, DTA; ( ), Ipser and Schuster [13].

## Acknowledgements

This research was funded by the National Science and Engineering Research Council of Canada through Grant No. A5113 to G.Y. Chao. We are also grateful to J.H.G. Laflamme of CANMET for help in synthesis and polished sections and to W.Bowman for the DTA. The first author wishes to thank the Korea Science and Engineering Foundation for financial assistance which enabled him to come to Ottawa to prepare this manuscript.

## References

1. Z.S. Medvedeva, M.A. Klochko, V.G. Kuznetsov and S.N. Andreeva, *Russian J. Inorg. Chem.*, **6**, 886(1961).
2. F.Grønvold and E. Røst, *Acta chem. Scand.*, **10**, 1620(1956).
3. C.A. Tibbals, Jr., *J. Amer. Chem. Soc.*, **31**, 902(1909).
4. L. Thomassen, *Z. Phy. Chem.*, **48**, 349(1929).
5. A. Kjekshus and W.B. Pearson, con. *J. Physics*, **43**, 438(1965).
6. E. Hoffman and W.H. MacLean, *Econ. Geol.*, **71**, 1461(1976).
7. R.P. Elliott, Construction of Binary Alloys, First Suppl., McGraw-Hill, New York, 735(1965).
8. M. El-Boragy and K. Schubert, *Z. Metallkunde*, **62**, 314(1971).
9. W. Wopersnow and K. Schubert, *J. Less-Common Metals*, **51**, P35(1977).
10. P. Matkovic and K. Schubert, *J. Less-Common Metals*, **58**, 39(1978).
11. L.J. Cabri, J.F. Rowland, J.H.G. Laflamme and J.M. Stewart, *Can. mineral.*, **17**, 589(1979).
12. G. Chattopadhyay, Y.J. Bhatt and S.K. Khera, *J. Less-Common metals*, **123**, 251(1986).
13. H. Ipser and W. Schuster, *J. Less-Common Metals* **125**, 183(1986).
14. L.J. Cabri, Platinum-Group Elements: Mineralogy, Geology, Recovery, *CIM Spec.* **23**, 188(1981).
15. P. Matkovic and K. Schuber, *J. Less-Common Metals*, **52**, 217(1977).
16. W.O.J. Groeneveld Meijer, *Amer. mineral.*, **40**, 646-657(1955).
17. V.S. Khar'kin, R.M. Imamov and S.A. Semiletov, *Kristallografiya*, **14**, 907(1969); *Sov. Phys.-Cryst.*, **14**, 779(1970).
18. S. Bhan and H. Kudielka, *Z. Metalkde.*, **69**, 333(1978).
19. L.E. Berlincourt, H.H. Hummel and B.J. Skinner, Platinum-Group Elements: Mineralogy, Geology, Recovery, *CIM Spec.*, **23**, 19(1981).
20. A.D. Genkin, N.N. Zhuravlev and E.M. Smirnova, *Zapiski Vses. Miner. Obshch.* **92(1)**, 33(1963).
21. G.A. Kingston, *Miner. Mag.*, **35**, 815(1966).
22. V.A. Kovalenker, A.D. Genkin, T.L. Evastgneeva and I.P. Laputina, *Amer. Mineral.*, **60**, 489(1975).
23. H. Ipser, *Z. Metalkde*, **73**, 151(1982).
24. C. Millika and O.M. Screedharan, *J. Mater. Sci. Letters* **5**, 915(1986).
25. L.J. Cabri and K.M. Pickwick, *Econ. Geol.*, **69**, 263(1974).